

Diffusion and aggregation of Ag_n -clusters ($n = 2-9$) on HOPG probed by fs-two-photon-photoemission

 U. Busolt^{1,a}, E. Cottancin², L. Socaciu³, H. Röhr³, T. Leisner⁴, and L. Wöste³
¹ Heinrich-Hertz-Institut für Nachrichtentechnik Berlin GmbH, Einsteinufer 37, 10587 Berlin, Germany

² Université Claude Bernard Lyon 1, Bâtiment Kastler, 69622 Villeurbanne Cedex, France

³ Fachbereich Physik, Freie Universität Berlin, Arnimallee 14, 14195 Berlin, Germany

⁴ Technische Universität Ilmenau, Institut für Physik, Weimarer Strasse 32, 98693 Ilmenau, Germany

Received 30 November 2000

Abstract. The diffusion and aggregation of preformed Ag_n -clusters ($n = 2-9$) deposited onto a highly oriented pyrolytic graphite (HOPG) substrate is studied by two-photon-photoemission (2PPE). The sample is irradiated with ultrashort laser pulse pairs and the kinetic energy of the emitted photoelectrons is analyzed in a magnetic bottle type time-of-flight spectrometer. During annealing of the sample from 100 K up to room temperature, nanoparticles are formed on the surface by diffusion and aggregation of the silver clusters. A steep increase of the total photoelectron yield at a sample temperature of about 150 K is explained by the excitation of plasmons in the silver nanoparticles. From the kinetic energy distribution of the photoelectrons we deduce a strong variation of the work function of the sample during the formation of the nanoparticles, which is attributed to a quantum size effect.

PACS. 68.43.Jk Diffusion of adsorbates, kinetics of coarsening and aggregation – 36.40.Sx Diffusion and dynamics of clusters – 78.67.-n Optical properties of nanoscale materials and structures – 36.40.Gk Plasma and collective effects in clusters

1 Introduction

2PPE is a widely used method to investigate the electronic structure of pure and adsorbate covered surfaces. It opens up the possibility to analyze the kinetic energy of the emitted photoelectrons as well as to conduct time-resolved measurements with femtosecond laser-pulses in order to get informations about the carrier dynamics [1–6]. The method is specially suited for cluster covered surfaces since it allows to analyze the influence of the morphology of the adsorbate on the excitation path.

It is well known that small silver clusters have a high mobility on HOPG-surfaces at room temperature (RT) [7]. To our knowledge no experiments, which investigate the temperature dependent coalescence of the silver clusters, exist so far. In earlier 2PPE-experiments [6] we observed the cluster size dependence of the 2PPE-spectra at a sample temperature of 100 K. The work function of the sample showed a pronounced odd/even effect, which is caused by the different charge transfer of odd- and even-numbered silver clusters to the substrate. From these observations we concluded that the clusters do not coalesce but retain their identity on the substrate at 100 K. The surface of the HOPG substrate is characterized by large flat terraces, which are separated by nearly parallel steps [8].

Scanning tunneling microscope (STM) measurements at RT revealed that silver clusters first diffuse across the terrace before they end up along the steps as the lower coordination number of C-atoms at the steps offer a stronger binding of the clusters [8].

The diffusion coefficient follows an Arrhenius law ($D = D_0 \exp(-E_a/kT)$) where E_a is the activation energy [9]. The earlier estimated activation energy of $E_a \geq 0.65$ eV for the diffusion of single Ag-adatoms on HOPG terraces [9] seems too high compared to new theoretical calculations for the binding energy of single Ag-adatoms on HOPG terraces of $E_b = 0.54$ eV as $E_b \geq E_a$ [10].

The growth of silver nanoparticles is detectable by a huge photoelectron yield of silver nanoparticles compared *e.g.* with a smooth silver surface [11–13]. The effect is based on the excitation of surface plasmons in the silver nanoparticles and depends on the used photon energy and the size of the nanoparticles [14–17].

For silver islands on HOPG a quantum size effect (QSE) was measured by one-photon-photoemission, where the signals reveal modulations *versus* the electron energy [7, 18]. The principal requirements [19] for the observation of a QSE are fulfilled for our system as well: (1) a mismatch of material properties at the interface in order to confine electrons in the adsorbate; (2) a very low roughness of the interface; (3) a large electron mean free path, which is greater than the film thickness. If in this case

^a e-mail: ulrike.busolt@hhi.de

the distance between the vacuum barrier and the adsorbate/substrate interface is comparable to the de Broglie wavelength of the electrons, electronic properties like the work function depend on the film thickness. Periodic oscillations of the work function as a function of the film thickness were already predicted 1976 by Schulte [20], who calculated the variations of the work function of jellium slabs surrounded by vacuum. The theoretical oscillation amplitude of the work function decreases from approximately 1 eV for 1 monolayer of metal to about 0.1 eV for 20 monolayers [20]. At the same time a stepwise increase of the density of states (DOS) at the Fermi level as a function of film thickness is predicted [21,22]. Measurements of periodical variations of the work function as a function of overlayer thickness were done for indium overlayers on a gold substrate [23].

It is to be expected that the reflection of the electrons at the adsorbate/substrate interface has an influence on the carrier relaxation dynamics in cases where the phase space for electron-electron scattering inside the adsorbate is reduced.

2 Experiment

The experiments were performed in an ultra-high-vacuum system with a background pressure of 5×10^{-10} mbar. Fig. 1 shows a scheme of the experimental setup. It allows to perform a soft-landing experiment with mass-selected cluster ions having a deposition energy considerably lower than the binding energy per atom of the cluster.

A cold-reflex discharge ion source (CORDIS) [24,25] was modified to yield four primary Xe^+ -ion beams of typically 15 kV and about 5 mA each. They are directed onto four water-cooled silver targets. The emerging clusters are collected by electrostatic fields and they are deflected into a large gas-filled ion guide, which serves to moderate and cool the ions by collision with He gas. The cluster ions are mass selected by a quadrupole mass filter and are guided into the UHV deposition chamber by another quadrupole ion guide where their kinetic energy is further reduced. Adjustable electrostatic lenses and a retarding potential at the sample serve to determine the kinetic energy distribution in the cluster beam. With this setup it is possible to achieve real soft landing conditions with deposition energies of 1 eV-2 eV/cluster. It is possible as well to deposit clusters with preselected high deposition energies and a narrow energy distribution. The cluster source provides a cluster beam between 700 pA for Ag_4 and 3 nA for Ag_3 .

The HOPG substrate is cleaved before insertion into the vacuum chamber. Under UHV conditions it is cleaned by flashing the sample rapidly to 1400 K by electron impact heating. The substrate is then cooled to liquid nitrogen temperatures. The temperature is measured near the sample at the lower part of the sample holder which is electrically isolated by means of sapphire crystals. This allows to monitor the deposition rates by measuring the cluster current on the sample. The distribution of the kinetic energy of the deposited clusters is controlled by monitoring

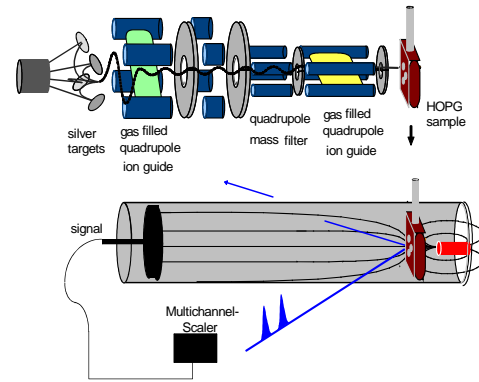


Fig. 1. Schematic diagram of the experimental setup (for details see main text.)

the current of the deposited ions as a function of the retarding potential applied to the substrate. The coverage of the sample was chosen to be equivalent to 4% of an atomic monolayer. The time for deposition depends on the cluster size.

We use a magnetic bottle type time-of-flight spectrometer which was introduced by Kruit and Read for gas-phase applications [26]. The instrument makes use of a strong diverging magnetic field to collect the photoelectrons and a weak guiding magnetic field, which directs the electrons through a flight tube to an electron multiplier (microsphere plate [27]). The strong field is produced by a small heatable permanent magnet (1 T) which is placed directly behind the HOPG substrate. The guiding field (1 mT) is produced by a coil. The whole electron spectrometer is surrounded by four Helmholtz coils for the compensation of external magnetic fields. The interior of the spectrometer is coated with graphite to ensure a homogeneous work function. An electron acceptance angle of about 2π is theoretically possible. The time-of-flight of the electrons is measured by a time-to-digital converter and later converted into the kinetic energy of the electrons. The calibration of the spectrometer is carried out by taking a series of photoelectron spectra of the pure graphite sample with different voltages applied to the sample.

The sample is irradiated under 45° by two subsequent fs laser pulses of 390 nm ($h\nu = 3.18$ eV) with an adjustable time delay. These pulses are produced by a laser system, that consists of a titanium sapphire oscillator which is pumped by a 9 W argon ion laser and of a Nd:YLF-pumped regenerative amplifier to produce ultrashort ($t < 100$ fs, 400 mJ/pulse) laser pulses with a repetition rate of 1 kHz. The pulses are frequency doubled in a BBO crystal. The beam is splitted into two pulses and one of them is delayed by a computer controlled delay line. The intensity of the light on the sample must be controlled carefully in order to avoid multiphoton processes and space charge broadening. Therefore the experiments were carried out with a pulse energy of below 500 nJ and a peak intensity of about 10^8 W/cm² as the spot size on the sample is about 1 mm². Both beams are *p*-polarized, *i.e.* with the electric field vector being parallel to the plane of

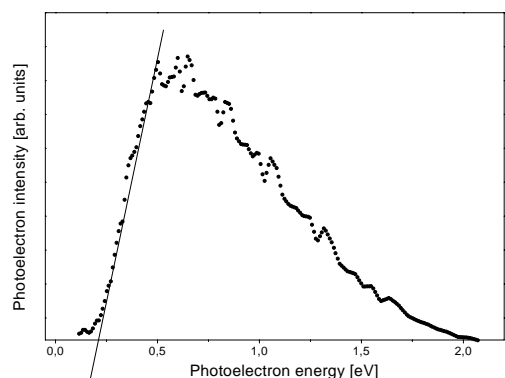


Fig. 2. 2PPE-spectrum for Ag_5 deposited on a HOPG substrate. The straight line indicates the energetic location of the low energy cutoff of the spectrum by extrapolation to the x -axis.

incidence. The 2PPE-spectra are taken with a fixed time delay between subsequent laser pulses.

3 Results and discussion

Fig. 2 shows a typical 2PPE-spectrum for Ag_5/HOPG at a sample temperature of 100 K. The shape of the spectrum is similar to the spectrum of pure HOPG and dominated by the influence of hot electrons. The straight line shows the energetic location of the low energy cutoff of the spectrum by extrapolation to the x -axis. Any modification of the energetic location of the low energy cutoff indicates a change of the work function of the sample [28,29].

Taking continuously 2PPE-spectra during annealing of the sample from 100 K up to RT with a heating rate of approximately 1 K/min leads to 3–4 spectra/K. Fig. 3a shows the resulting total photoelectric yield of one series of measurements for Ag_6/HOPG , integrated over all electron energies, as a function of the measured temperature. The temperature is subject to an error of about ± 5 K as it is measured at the sample holder and not directly at the sample surface itself and therefore it depends on the heating rate. A steep increase of the photoelectron yield is visible at 155 K. This increase shows, that the plasmon resonance of the grown nanoparticles begins to shift into the photon energy. The excitation path changes compared to the low temperature regime [6], where the first photon is absorbed by the substrate. With the formation of silver nanoparticles the predominant part of the signal results from absorption of both photons inside the adsorbate. The signal of the pure HOPG is not subtracted, but equivalent measurements of the pure HOPG-substrate show that this signal is very low.

Fig. 3b shows the changes of the work function of the sample, referred to the work function at 100 K, deduced from the low energy cutoff of the spectra. Distinct variations of the work function of about 0.2 eV are detectable at temperatures lower and equal to the excitation of the surface plasmon of the silver nanoparticles. The amount of silver on the surface does not change and if the formation of the nanoparticles is finished, the thickness of

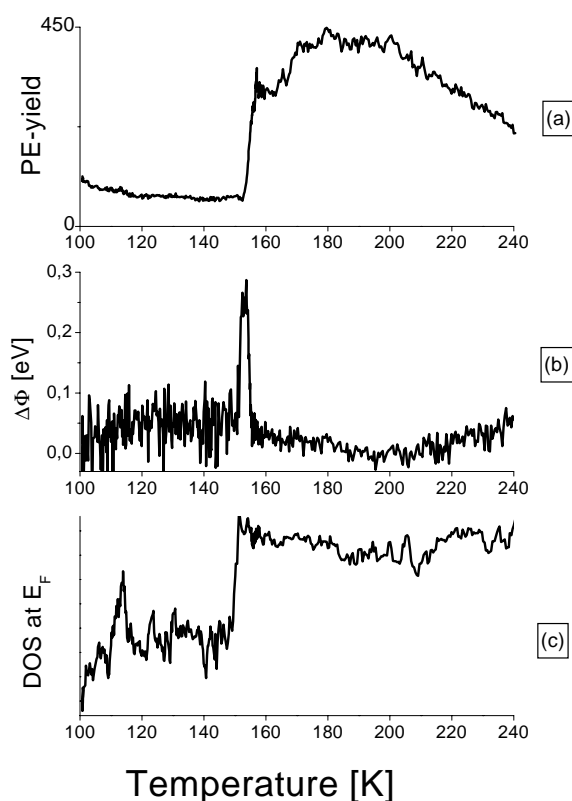


Fig. 3. (a) Shows the total photoelectric yield for Ag_6/HOPG , integrated over all photoelectron energies, as a function of the substrate temperature. (b) Variation of the work function of the sample, referred to the value at $T = 100$ K. (c) DOS at the Fermi level, referred to the value at $T = 100$ K.

the nanoparticles does not change with temperature. This is the reason why the work function does not show any further oscillations.

Fig. 3c shows the changes of the DOS near the Fermi level of the sample, deduced by linear extrapolation of the high energy cutoff of the 2PPE-spectra and referred to the value at 100 K. The DOS increases stepwise at around 150 K, just before the increase of the photoemission yield. This effect is only detectable, because the DOS of the HOPG-substrate is vanishingly low at the Fermi level. Therefore every increase of the DOS of the adsorbate near the Fermi level becomes apparent.

Similar experiments were repeated for the different cluster sizes $n = 2-9$. As an example Figs. 4a-c shows the result for Ag_9/HOPG . Although one might expect cluster size dependent differences concerning the temperature, at which the increase of the photoyield takes place, we are not able to detect them. This could be due to the fact, that the shift of the plasmon resonance into the photon energy does not take place until the clusters are aggregated.

4 Summary

We observe the coalescence of small mass-selected silver clusters by the appearance of their plasmon absorption in

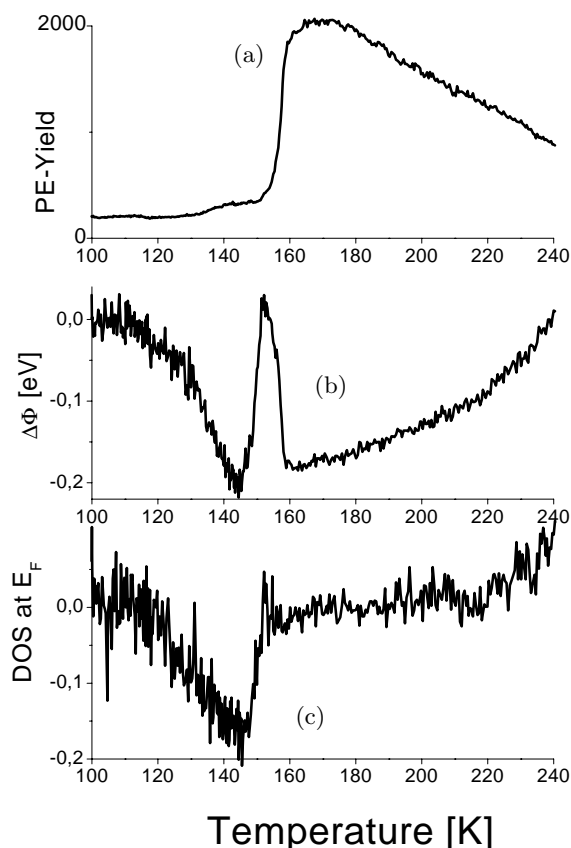


Fig. 4. (a) Shows the total photoelectric yield for Ag_9/HOPG , integrated over all photoelectron energies, as a function of the substrate temperature. (b) Variation of the work function of the sample, referred to the value at $T = 100$ K. (c) DOS at the Fermi level, referred to the value at $T = 100$ K.

the 2PPE-spectra. Below the coalescence temperature we find a strong variation of the work function of the sample, which we attribute to a QSE in the so formed adsorbate islands.

No influence of the initial cluster size has been detected on the coalescence temperature. This is probably not surprising, since these effects appear with larger nanoparticles at a temperature where every information about the initial cluster size is already lost.

This work was supported by the Deutsche Forschungsgemeinschaft (Sfb 450) and by the Alexander-von-Humboldt-Stiftung. The authors would like to thank Prof. Dr. K.-H. Meiwes-Broer, Prof. Dr. G. Gerber, Dr. W. Harbich, Dr. W. Pfeiffer and Dr. W. Christen for stimulating discussions.

References

1. E.W. Plummer, W. Eberhardt, *Adv. Chem. Phys.* **49**, 533 (1982).
2. T. Fauster, W. Steinmann, *Two-photon photoemission spectroscopy of image states in photonic probes of surfaces*, edited by P. Halevi (Elsevier, Amsterdam, 1995), p. 347.
3. R. Haight, *Surf. Sci. Rep.* **8**, 275 (1995).
4. C.B. Harris, N.-H. Ge, R.L. Lingle Jr, J.D. McNeill, C.M. Wong, *Ann. Rev. Phys. Chem.* **48**, 711 (1997).
5. H. Petek, S. Ogawa, *Progr. Surf. Sci.* **56**, 239 (1998).
6. U. Busolt, E. Cottancin, H. Röhr, L. Socaciu, T. Leisner, L. Wöste, *Eur. Phys. J. D* **9**, 523 (1999).
7. F. Patthey, W.-D. Schneider, *Phys. Rev. B* **50**, 17560 (1994).
8. G.M. Francis, L. Kuipers, J.R.A. Cleaver, R.E. Palmer, *J. Appl. Phys.* **79**, 2942 (1996).
9. E. Ganz, K. Sattler, J. Clarke, *Surf. Sci.* **219**, 33 (1989).
10. D.M. Duffy, J.A. Blackman, *Surf. Sci.* **415**, L1016 (1998).
11. V.M. Shalaev, C. Couketis, T. Haslett, T. Stuckless, M. Moskovits, *Phys. Rev. B* **53**, 11193 (1996).
12. J.T. Stuckless, M. Moskovits, *Phys. Rev. B* **40**, 9997 (1989).
13. F. Sabary, J.C. Dudek, H. Bergeret, *J. Appl. Phys.* **70**, 1066 (1991).
14. T. Tsang, T. Srinivasan-Rao, J. Fischer, *Opt. Lett.* **15**, 866 (1990).
15. P. Monchicourt, M. Raynaud, H. Saringar, J. Kupersztych, *J. Phys.: Cond. Matt.* **9**, 5765 (1997).
16. J. Bosbach, D. Martin, F. Stietz, T. Wenzel, F. Träger, *Appl. Phys. Lett.* **74**, 2605 (1999).
17. T. Wenzel, J. Bosbach, F. Stietz, F. Träger, *Surf. Sci.* **432**, 257 (1999).
18. G. Neuhold, *Über die Valenzbandstruktur epitaktischer Metallfilme* (Wissenschaft und Technik, 1996).
19. C. Marlière, *Surf. Sci.* **269/270**, 777 (1992).
20. F.K. Schulte, *Surf. Sci.* **55**, 427 (1976).
21. J.C. Boettger, S.B. Trickey, *Phys. Rev. B* **45**, 1363 (1992).
22. I.P. Batra, S. Ciraci, G.P. Srivastava, J.S. Nelson, C.Y. Fong, *Phys. Rev. B* **34**, 8246 (1986).
23. C. Marlière, *Thin Solid Films* **136**, 1192 (1990).
24. T. Leisner, Ch. Rosche, S. Wolf, F. Granzer, L. Wöste, *Surf. Rev. Lett.* **3**, 1105 (1996).
25. R. Keller, F. Nöhmayer, P. Spädke, M.-H. Schönenberg, *Vacuum* **34**, 31 (1984).
26. P. Kruit, F.H. Read, *J. Phys. E* **16**, 313 (1983).
27. A.S. Tremsin, J.F. Pearson, J.E. Lees, G.W. Fraser, *Nucl. Instrum. Meth. Phys. Res. A* **368**, 719 (1996).
28. G. Ertl, J. Küppers, *Low energy electrons and surface chemistry* (VCH Verlagsgesellschaft mbH, 1985).
29. A. Goldmann, Photoelectron spectroscopy, in: *Thin metal films and gas chemisorption*, edited by P. Wissmann (Elsevier, 1987), p. 160.